Susceptibility of SiO_2, ZrO_2, and HfO_2 Dielectrics to Moisture Contamination

Prashant Raghu, Chris Yim, and Farhang Shadman
Dept. of Chemical Engineering, University of Arizona, Tucson, AZ 85721

Eric Shero
ASM America, Phoenix, AZ 85034

DOI 10.1002/aic.10148
Published online in Wiley InterScience (www.interscience.wiley.com).

Moisture contamination of HfO_2 and ZrO_2 ultrathin dielectric films, deposited by atomic layer chemical vapor deposition (ALCVD™), is investigated and compared to that of native SiO_2. Results show that HfO_2 and ZrO_2 surfaces adsorb higher amounts of moisture and bind moisture more strongly than SiO_2 surfaces. A multilayer model is developed to represent the dynamics of moisture interaction with these three oxides. Using this model, the fundamental kinetic parameters are determined. The adsorption rate constants are of the same order of magnitude for all three surfaces. However, the desorption rate constants for ZrO_2 and HfO_2 are almost three orders of magnitude lower than that for SiO_2. Activation energies for desorption of water molecules from the first two layers are 33, 27, and 19 kJ/mol, for ZrO_2, HfO_2, and SiO_2, respectively. Results obtained in this study suggest that the HfO_2 and ZrO_2, as the new dielectric materials, are more prone to moisture contamination than SiO_2.
AIChE J, 50: 1881–1888, 2004
Keywords: adsorption, outgassing, moisture, hafnium dioxide, zirconium dioxide

Introduction

The International Technology Roadmap for Semiconductors suggests that silicon dioxide (SiO_2) will soon reach its intrinsic limits as a gate dielectric material for future MOSFET (n-type metal oxide semiconductor field-effect transistor)–based devices. As feature size shrinks, films of SiO_2 for gate dielectrics will be so thin that electron tunneling through the dielectric layer will prevent their use (Lo et al., 1997). To maintain high drive current, while minimizing leakage current, low equivalent oxide thickness is achieved by using materials with higher dielectric constant (high-*k* dielectrics). Among the high-*k* materials, hafnium dioxide (HfO_2) and zirconium dioxide (ZrO_2) with dielectric constants of about 22–23 are promising candidates. They have reasonably large bandgaps and exhibit excellent electrical characteristics (Conley et al., 2001; Kang et al., 2000; Lee at al., 2000). According to thermodynamic calculations, these oxides form a short list of candidate metal oxides that are stable in contact with silicon (Balog et al., 1977). This stability, along with stability in contact with gate materials, is critical for successful integration into silicon metal oxide semiconductor (MOS) technology.

Moisture is a ubiquitous impurity and a contaminant that is becoming increasingly more critical during the fabrication and application of thin films. Moisture contamination can cause various problems such as haze formation, change in adhesion properties of surfaces, and particle formation. The presence of moisture also results in corrosion of components in reactive gas systems, unintentional oxidation of various thin films, and changes in selectivity and rates of processes, such as gaseous oxide etching. It is also the most difficult impurity to control because of its abundance in all environments, small size, high polarity, and ability to hydrogen bond.

Wafers are inevitably exposed to the molecular contaminants

Correspondence concerning this article should be addressed to P. Raghu at prashant@email.arizona.edu.

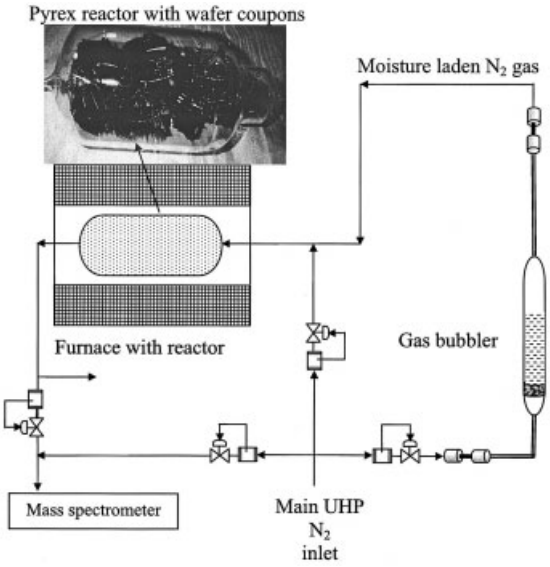

Figure 1. Experimental setup.

present in the cleanroom environment during processing of semiconductor devices. Moisture is known to adsorb readily on Si and SiO_2 surfaces (Sneh et al., 1995). Moisture contamination affects optical thickness measurement of ultrathin films. It results in an apparent increase in the film thickness, thereby deteriorating the precision performance of ellipsometers. Rana et al. (2002) assert that moisture also aggravates organic contamination of these surfaces. Therefore, moisture contamination of wafer surfaces during critical processing steps such as gate stack formation can be detrimental. It can lead to degradation of gate oxide quality, resulting in deterioration of device performance. Adsorption of high levels of moisture on the new high-*k* gate dielectric surfaces can result in problems like adhesion of films for gate stack formation. It is known that moisture diffuses through ultrathin HfO_2 and ZrO_2 films, reacts with silicon at the interface, and forms SiO_2 or silicate, resulting in lowering of the overall dielectric constant (Morita et al., 1985).

The interaction of moisture with ZrO_2 and HfO_2 surfaces is also important in other areas besides gate dielectric application. These oxides are used as barrier layers for superconductors, as laser optic, biomedical, and prosthetic coatings. Hence, characterization of their adsorption behavior is critical. The adsorption/desorption characteristics of trace [parts-per-billion (ppb)] levels of moisture on SiO_2, HfO_2, and ZrO_2 were previously reported (Raghu et al., 2003; Rana et al., 2003). However, moisture concentrations are known to range from the high ppm to low percentage levels in a typical ambient clean room. Therefore, the main objective of this study is to compare the behavior of SiO_2, HfO_2, and ZrO_2 surfaces exposed to high moisture concentrations. This study offers a direct comparison of the extent and the energetics of moisture contamination on the three oxide surfaces. The results of this work will aid in the selection of the most appropriate dielectric film and in the design of related process tools and techniques.

Experimental

Figure 1 shows a schematic of the experimental setup and the reactor used for this study. HfO_2 and ZrO_2 films were deposited on as-received 8-in. p-type, 10–80 Ω-cm, Czochralski (Cz) grown double-sided, polished, (100)-oriented silicon wafers. HfO_2 and ZrO_2 films were deposited by atomic layer chemical vapor deposition (ALCVD™) at 300°C using $HfCl_4$ and $ZrCl_4$, respectively, as precursors in a cross-flow, isopressure Pulsar® 2000 reactor. The pressure was maintained below 10 Torr. The films were grown by repeated pulse–purge cycles of precursors using N_2 as the carrier gas. The thickness of the films was 50 Å. TEM and XRD results indicated that HfO_2 was amorphous, whereas ZrO_2 was polycrystalline with mostly tetragonal crystallites. The films were not subjected to any postdeposition treatment before adsorption/desorption experiments. Studies on SiO_2 were performed on native oxide grown on Si (100). The wafers were diced to produce 2 × 1-cm coupons that were loaded on nickel-coated stainless steel springs. The total number of wafer coupons used was approximately 700. The loaded springs were packed inside a reactor to give a high sample surface area. The ratio of the sample surface area to the glass reactor area was 6:1. The volume of the reactor was 888 cm^3.

All portions of the stainless steel gas-delivery system were maintained at 65°C to reduce the memory effect associated with the adsorption and desorption of moisture. The entire setup was designed to minimize the dead volumes in the lines, components, reactor, and monitoring systems. Moisture, the impurity of interest, was introduced into the challenge stream by a gas bubbler. A separate ultrapure N_2 stream was used for dilution; the moisture concentration was controlled by adjusting the purge flow rate, using mass flow controllers. Moisture concentration in the reactor outlet stream was monitored using an electron impact mass spectrometer (EIMS) with ppb level detection limit. Ultrapure N_2, as zero gas, was used for preparing calibration mixtures and for diluting the sample gas; that would reduce the moisture concentration below 300 ppm, which was the upper limit of the EIMS range. Moisture levels in the ultrapure N_2 gas were $<$500 ppb.

The experimental procedure consisted of the following three steps: (1) initial purge and bake under ultrahigh purity (UHP) N_2 at 350°C, (2) isothermal adsorption of moisture by exposure of the reactor to impurity-laden N_2 gas, and (3) isothermal desorption under N_2. Moisture concentration in the outlet of the reactor was the primary variable monitored during each experimental run.

Results and Discussion

Figure 2 shows the outlet–gas moisture concentration profile during the three cycles for a 0.3% moisture exposure. Based on the noise level of the mass spectrometer raw data, the overall error in the experimental data was less than 5%. The amount of moisture adsorbed on the surface is calculated from the area above the adsorption temporal profile. Similarly, the area under the desorption curve is a measure of the total amount of moisture desorbed during the isothermal N_2 purge. The total amounts of moisture adsorbed on SiO_2, HfO_2, and ZrO_2 when exposed to 0.3% moisture at different temperatures are plotted in Figure 3. At any given temperature, the moisture adsorption capacity of ZrO_2 and HfO_2 is higher than that of SiO_2. This trend is similar to results on moisture contamination in ppb levels (Rana et al., 2003). The moisture adsorption loading density is several times higher than the site density. This

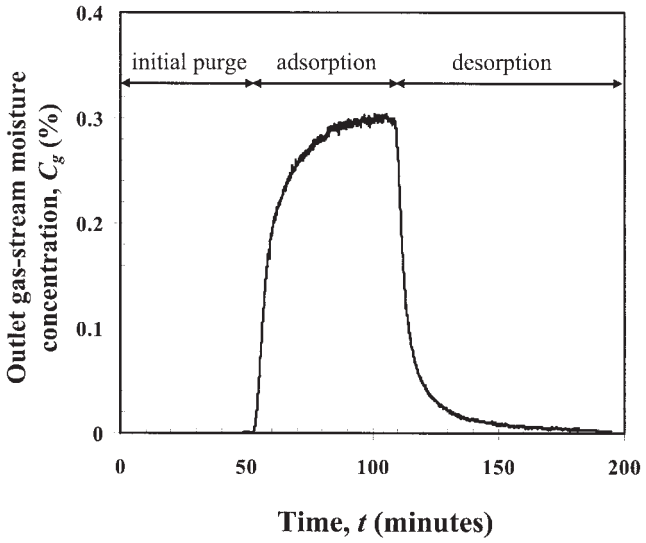

Figure 2. Outlet–gas moisture concentration profile during adsorption of 0.3% moisture on ZrO_2 at 24°C.

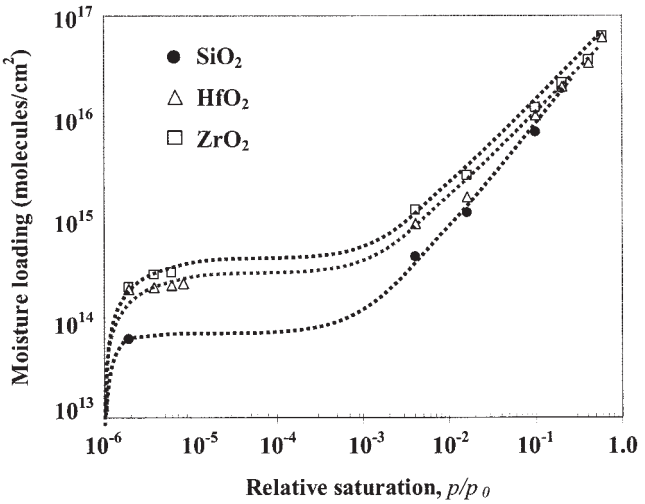

Figure 4. Effect of challenge concentration on moisture loading on SiO_2, HfO_2, and ZrO_2 at 24°C.

The solid lines are drawn through the data points to show the trend.

indicates that moisture adsorption occurs in multiple layers. Moisture chemisorbs dissociatively on SiO_2 and most metal oxides to form tightly bound surface hydroxyl groups (Anderson et al., 1964; Peri et al., 1968; Sindorf et al., 1983; Sneh et al., 1995, 1996; Takeda et al., 1999). Moisture can also stack on top of these surface species to form multiple layers of weakly physisorbed molecules.

The higher adsorption loading on HfO_2 and ZrO_2 is attributed to their higher polarity and higher site density. The metal–oxygen bonds in HfO_2 and ZrO_2 are more polar than those in SiO_2 (Takeda et al., 1999). Therefore, moisture is more attracted to HfO_2 and ZrO_2 than to SiO_2. On a thermally grown oxide on Si (100), the number of hydroxyl groups formed is reported to be about 4.6×10^{14} per cm^2 (Sneh et al., 1995). In the case of porous ZrO_2 particles, the surface density of hydroxyl groups has been reported to be 1.0×10^{15} per cm^2 (Takeda et al., 1999). No such data were available for HfO_2 at the time of this study. The higher adsorption on ZrO_2 could also be attributed to the larger number of sites available for adsorption. It should be noted that the adsorption/desorption loading and kinetics depend on the type of oxide and its state of crystallinity. The values reported here are specific to amorphous SiO_2 and HfO_2, and polycrystalline ZrO_2. It is generally believed that polycrystalline films have higher surface area per unit geometric area of the sample.

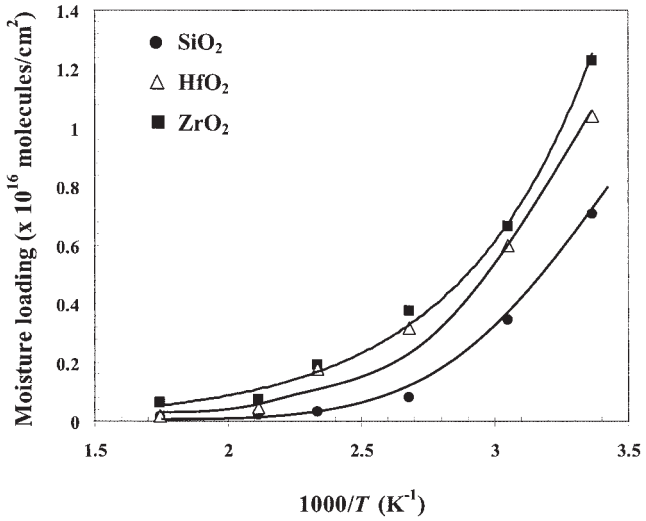

Figure 3. Comparison of moisture loading on SiO_2, HfO_2, and ZrO_2 for 0.3% challenge.

The solid lines are drawn through the data points to show the trend.

Experiments were also performed with wafer surfaces exposed to varying moisture concentrations. Figure 4 summarizes the effect of moisture challenge concentration on loading for SiO_2, HfO_2, and ZrO_2 surfaces at 24°C. The chart also includes low concentration (ppb level) data obtained in a separate study performed by Rana et al. (2003). The plot indicates a type II adsorption isotherm, similar to those predicted by the Brunauer–Emmett–Teller (BET) model. The amount of adsorbed moisture increases significantly as moisture challenge concentration approaches the saturation pressure. However, the difference in moisture loadings on the three surfaces reduces at higher concentrations. As loading increases, the surface is covered with more layers of physisorbed moisture; the adsorption thereafter becomes independent of the nature of the surface. This explains why the oxides have similar adsorption capacities at high exposure levels.

The relative affinity of the three surfaces to moisture can also be evaluated by comparing the adsorption/desorption kinetics. Figure 5 compares the moisture adsorption/desorption kinetics on the three surfaces at 24°C for a gas-phase moisture concentration of 0.3%. The results clearly show the differences in the equilibrium adsorption loadings on the three oxide surfaces. The SiO_2 surface is equilibrated faster than HfO_2 and ZrO_2 surfaces, as seen from the plot. The rate of desorption is also faster on SiO_2. This trend is generally observed at all temperatures and gas-phase moisture concentrations studied here.

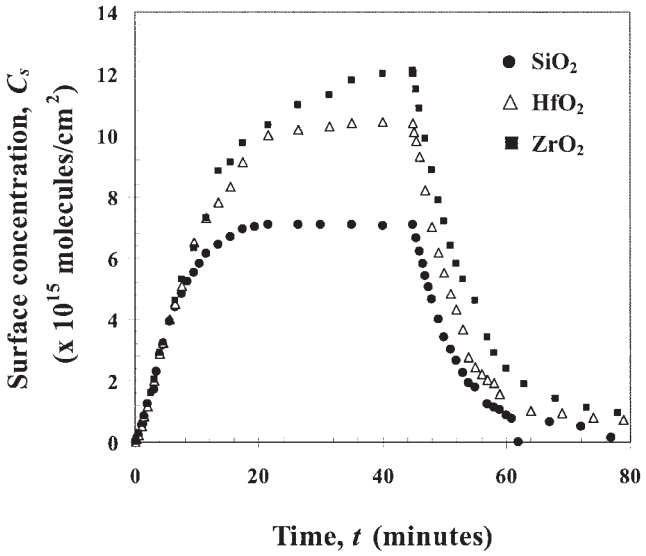

Figure 5. Comparison of adsorption/desorption kinetics of moisture on SiO_2, HfO_2, and ZrO_2 at 24°C for 0.3% moisture exposure.

Multilayer Adsorption Model

It is generally accepted that oxide surfaces adsorb multiple molecular layers of moisture at room temperature and at exposures far below the saturation pressure of moisture. There is some disagreement on the total amount of physisorbed moisture reported at a given temperature, primarily because of varying analytical techniques and detection levels. However, it is collectively agreed that physisorption occurs upon the first hydroxylated layer. The physisorption in this first layer is facilitated through hydrogen bonding with surface hydroxyl groups. Additional water molecules can adsorb on top of each other to form multiple layers, as illustrated in Figure 6. These water molecules are held together by weak van der Waal's forces of attraction. The number of monolayers formed is a function of temperature, level of exposure, and nature of the surface. The loading values obtained in the present study definitely indicate that multiple layers of physisorbed moisture are formed on all three surfaces.

Moisture adsorption on a hydroxylated surface is highly activated. Silanol (Si–OH) surface groups are highly acidic (Sneh et al., 1995). Various isoelectric points between pH values of <1 and 4.5 have been measured for hydroxylated surfaces (Iller, 1979). The Si–OH$\cdots$H$_2$O interaction exceeds typical hydrogen bond strengths. One possible explanation is a partial $SiO^-\cdots H_3O^+$ ionic interaction (Anderson et al., 1968; Frpiat et al., 1965). The ability of SiOH groups to donate a proton to H_2O and organic bases has been suggested as an explanation for the conductivity of hydroxylated SiO_2 surfaces. According to Vanquickenborne (1991), additional evidence for strong Bronsted acidity is the lack of affinity of SiOH species for strong inorganic acids such as HF. Sneh et al. (1996) reported that moisture adsorbs on fully hydroxylated SiO_2 surface with a desorption activation energy of about 84 kJ/mol at zero coverage as a consequence of the acidic nature of the surface. A hydroxylated surface can be as reactive as the bare oxide itself. Because of the partial $SiO^-\cdots H_3O^+$ ionic interaction, water adsorption even on the second monolayer is expected to be more activated than the H_2O–H_2O interactions between molecules adsorbed in higher layers.

Based on these observations, a fundamental model is developed to represent the mechanism and to quantify the kinetics of adsorption of moisture on the oxide surfaces. Molecules close to the surface are tightly bound to the surface. The molecules adsorbed in the higher layers are relatively loosely bound to each other. As the adsorption proceeds to higher layers, the overall activation energy of desorption will appear lower than that observed initially for molecules closer to the surface. The model differentiates the adsorbed H_2O molecules into two types: (1) molecules in the first two layers that are influenced by the oxide surface forces and interactions and (2) molecules in layers 3 and above that are screened from the surface. The two key assumptions in the development of the model are: (1) all sites are identical and (2) the lateral interactions among adsorbed molecules are negligible.

According to the above mechanistic model, the net rate of adsorption at any time is given by

$$R_a = k_a C_g \tag{1}$$

The rate coefficient k_a is independent of the gas-phase concentration (C_g), but depends on the surface coverage. The process steps representing adsorption and desorption on different layers are simultaneous and not completely sequential (similar to the assumption in the BET model). However, unlike the BET model, which is limited to predicting only equilibrium isotherms, the present model does not assume equilibrium condition. It gives the dynamics of adsorption and desorption processes as well as the equilibrium. At any time, the surface consists of two types of sites: the sites under the surface influence (first and second layers) and the higher-level sites. The assumption of two levels of energetics for the adsorption process is also similar to the one in the BET model, except that the surface interaction in this case is extended to both bare surface and hydroxylated surface; other layers will experience only water–water interactions. Therefore, the apparent rate coefficient (the average observed value) would depend on surface coverage, starting with a value of k_{a1}, corresponding to the adsorption on sites influenced by surface interactions, and

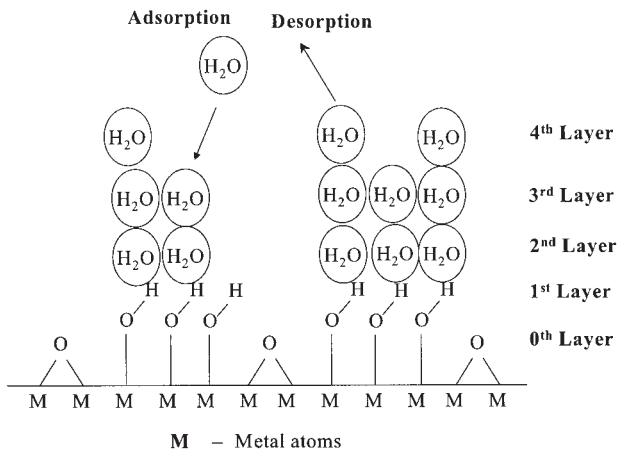

Figure 6. Multilayer formation on oxide surfaces.

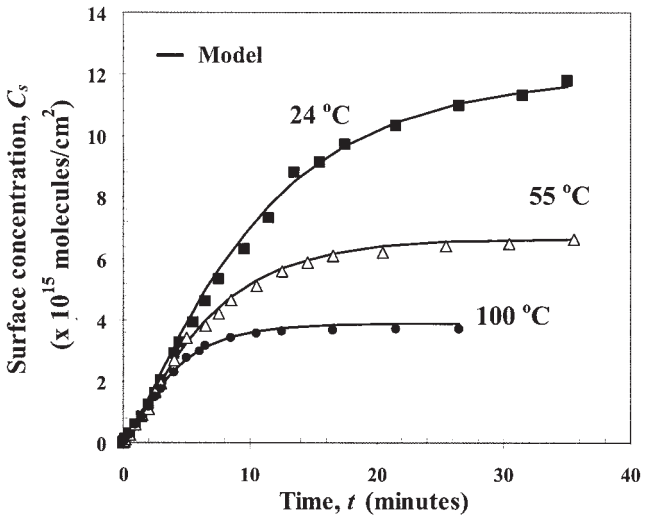

Figure 7. Fit of the model to the experimental adsorption data on ZrO_2 at different temperatures.

gradually changing and approaching a final value of k_{a2}, corresponding to adsorption of water on other water molecules without surface influence. The nature of this variation is complex; in this model it is represented by the following semiempirical equation

$$k_a = k_{a1} + (k_{a2} - k_{a1}) \frac{\theta}{(\theta + 1)} \tag{2}$$

where θ is the surface coverage, in equivalent number of monolayers, defined as

$$\theta = C_s/C_{s0} \tag{3}$$

where C_s is the surface concentration (in units of molecules/cm^2) and C_{s0} is the surface concentration to form a monolayer. Equation 2 agrees with the experimental data and shows the right observed limits as well as the right slope at the low moisture coverage.

Similarly, the rate of desorption is given by

$$R_d = k_d C_s \tag{4}$$

where the coefficient for desorption is

$$k_d = k_{d1} + (k_{d2} - k_{d1}) \frac{\theta}{(\theta + 1)} \tag{5}$$

κ_{d1} represents the desorption rate constant of water molecules influenced by surface interactions and k_{d2} denotes the desorption rate constant of water molecules shielded from the surface.

The overall process can be represented by the following mass balance

$$\frac{dC_s}{dt} = k_a C_g - k_d C_s \tag{6}$$

An optimization algorithm based on a combination of Gauss–Newton and quasi-Newton methods for constrained problems is used to fit the differential equations to the data and determine the model parameters (k_{a1}, k_{a2}, k_{d1}, and k_{d2}). Figure 7 shows the experimental data and the model-predicted surface concentration profiles for the adsorption of moisture on ZrO_2. The data shown are for a moisture challenge concentration of 0.3% at a flow rate of 200 cm^3/min. The model gives an excellent fit to the experimental data at different temperatures. Figure 8 depicts the model fit to experimental desorption data for ZrO_2 at different temperatures. Similar plots are obtained for SiO_2 and HfO_2, but are not presented here. The four rate constants are estimated at each temperature for the three oxides under consideration.

The rate parameters estimated from the model for all three surfaces are given in Table 1. Figure 5 shows the adsorption temporal profile of the three oxides. The initial slope of the curve, dominated by adsorption kinetics, is very similar for the three oxides. This is in agreement with the model predictions, which indicate that the values of k_{a1} and k_{a2} for the three oxides are very similar. As the adsorption process proceeds, simultaneous desorption becomes more important. The observed rate is then a net combination of adsorption and desorption and its average value is higher for ZrO_2 and HfO_2, compared to that for SiO_2. Desorption rate constants k_{d1} and k_{d2} of HfO_2 and ZrO_2 are lower than those of SiO_2; this suggests that the high-k materials have higher affinity for moisture compared to SiO_2. This higher affinity is attributed to their higher polarities. Molecules in the first two layers are strongly bound to the surface. They have lower rates of desorption compared to the molecules in the higher layers. Therefore, for all three surfaces, k_{d1} is smaller than k_{d2}. The desorption rate constant (k_{d2}) of molecules in higher layers is of the same magnitude on all three surfaces because these molecules do not experience any significant surface influence.

The values of rate constants at different temperatures are used to determine the activation energies for the adsorption and desorption process steps for each oxide. Figure 9 shows the

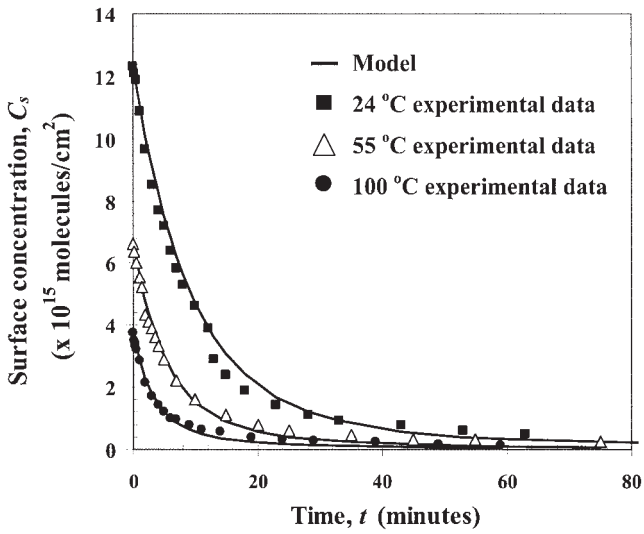

Figure 8. Fit of the model to experimental desorption data on ZrO_2 at different temperatures.

Table 1. Rate Constants (at 24°C) Determined by Fitting the Model to the H_2O Adsorption Data

Type of Moisture	Symbol	Unit	SiO_2	HfO_2	ZrO_2
1	k_{a1}	cm/min	5.20×10^{-3}	6.20×10^{-3}	6.50×10^{-3}
(tightly bound to surface)	k_{d1}	1/min	9.10×10^{-2}	3.20×10^{-4}	1.50×10^{-4}
2	k_{a2}	cm/min	1.50×10^{-2}	1.82×10^{-2}	1.70×10^{-2}
(screened from surface)	k_{d2}	1/min	1.45×10^{-1}	1.30×10^{-1}	1.08×10^{-1}

Arrhenius plot of desorption constants for ZrO_2; the activation energies are listed in Table 2. Desorption energy, E_{d1}, is highest at 33 kJ/mol for ZrO_2 surface, indicating that it has the highest affinity for moisture among the three oxides. The desorption energy (E_{d2}) for water molecules in higher layers is lower than E_{d1}, for all three oxides. All three oxides have similar values of E_{d2}. This is expected, given that this activation energy (E_{d2}) is a measure of only H_2O–H_2O interactions and independent of the surface type. However, the values obtained in this study are much lower than the H_2O condensation energy of 48 kJ/mol (Sneh et al., 1996). This is consistent with the model presented here because the desorbing surface molecules have fewer H_2O neighbors and therefore can desorb more easily compared to water molecules in bulk water. The activation energy of adsorption is low for all layers (both E_{a1} and E_{a2}). This is attributed to the fact that the adsorption process does not involve any energetic molecular rearrangements.

Using the values of k_{d1} and k_{d2}, the apparent activation energy of desorption (E_d) of moisture is computed from Eq. 5 for different surface coverages (θ). Figure 10 plots the dependency of E_d on θ for the three oxides. For each oxide, the apparent activation energy starts with a value close to that of E_{d1} at low values of θ and gradually approaches that of E_{d2} as θ increases. At very low surface coverages, the apparent activation energy of desorption is influenced only by surface interactions. As θ increases, H_2O molecules stack on the top of each other. The overall desorption rate is also influenced by H_2O–H_2O interactions. Hence, for all three surfaces E_d decreases as θ increases until it approaches E_{d2}, where desorption has no surface influence. For HfO_2 and ZrO_2, the decrease in E_d is sharper and E_d approaches E_{d2} when θ increases to a monolayer. For SiO_2, however, the decrease in E_d is gradual and the transition occurs at a higher value of θ. The arrangement of adsorbed H_2O molecules is different for all three surfaces and is governed by its surface chemistry. Experimental data and model results suggest that HfO_2 and ZrO_2 have higher affinity for moisture than SiO_2. Therefore, for a given surface coverage, HfO_2 and ZrO_2 are expected to have more molecules of type 1 (those influenced by the surface). This postulate is further supported by ppb-level moisture adsorption studies reported by Rana et al. (2003). It is reported that 45–50% of the adsorbed moisture is desorbed from SiO_2 surfaces using an isothermal N_2 purge at 30°C, whereas only 20–30% is removed from ZrO_2 surfaces. Most of the water molecules desorbed isothermally at 30°C would be weakly physisorbed molecules, predominantly in the higher layers, because they are much easier to desorb than those close to the surface. Because a lower portion of the total adsorbed moisture was removed during the low temperature purge from ZrO_2 surfaces, the fraction of the total molecules of type 1 is higher compared to that on SiO_2. Therefore, the presence of small amounts of adsorbed moisture should result in a drastic change in the nature of HfO_2 and ZrO_2 surfaces. Hence, the apparent activation energy of desorption decreases sharply as θ increases from zero. For SiO_2, however, the fraction of total adsorbed molecules of type 1 is lower than that for HfO_2 or ZrO_2. Therefore, a relatively higher surface coverage is required to alter the nature of the SiO_2 surface. Thus, E_d decreases at a higher value of θ for SiO_2. The proposed model does not consider lateral interactions between adsorbate molecules. The experimental results on the behavior of E_d, shown in Figure 10, validate this assumption. The presence of lateral attraction would result in an initial increase in E_d as θ increases from zero. In that case, a peak in E_d would be observed instead of a monotonous decrease, as shown in Figure 10.

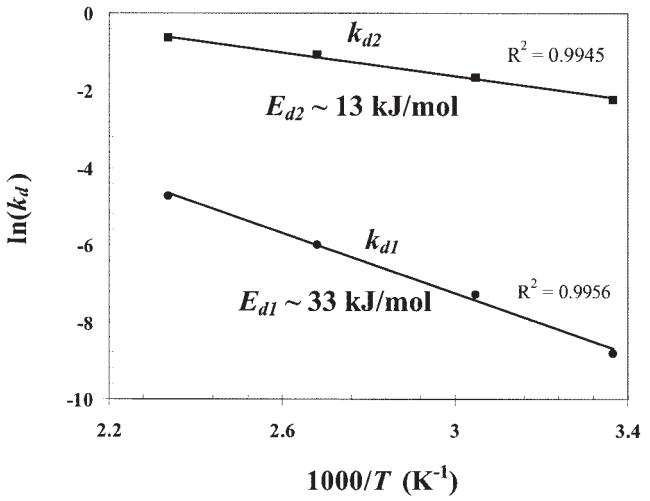

Figure 9. Arrhenius plot for desorption rate constants (k_{d1} and k_{d2}) for ZrO_2.

The results obtained in this study show that the "observed activation energy," which is an average property, depends on the extent of coverage and the distribution of adsorbed molecules among different layers. This is probably the main reason for the discrepancies among the values of activation energies reported in the literature. The activation energy of desorption of water from silica surfaces has been reported from a low value of 17.0 kJ/mol, by Dultsev et al. (1991), to as high as 68.2 kJ/mol reported by Young et al. (1960). These numbers seem low when compared to those reported by Sneh et. al. (1996), who studied submonolayer moisture adsorption on SiO_2 surfaces at subzero temperatures using LITD (laser-induced thermal desorption). They reported that H_2O adsorbs on fully hydroxylated SiO_2 surface with a desorption activation energy starting at a value as high as 84 kJ/mol as surface coverage approaches zero. BET isothermal adsorption experiments using gravimetry on fully hydroxylated silica surfaces have measured desorption energies of 50–72 kJ/mol (Zaborski et al., 1989). These studies report values determined under

Table 2. Activation Energies Estimated from Arrhenius Plots

Type of Moisture	Symbol	Unit	SiO_2	HfO_2	ZrO_2
1	E_{a1}	kJ/mol	~0	~0	~0
(tightly bound to surface)	E_{d1}	kJ/mol	19	27	33
2	E_{a2}	kJ/mol	~0	~0	~0
(screened from surface)	E_{d2}	kJ/mol	13	13	13

different experimental conditions such as surface preparation, temperature, pressure, surface analysis method, and surface coverage. Empirical factors such as sticking coefficients are very often used to estimate activation energies. The present study, however, takes a more fundamental approach and gives the intrinsic activation energies for each type of molecule and the dependency of the average activation energy on coverage.

The multilayer model not only provides a mechanistic description of the process and explanation of the experimental results, but also is a useful quantitative tool for predicting the amount of moisture that is adsorbed on a surface when it is exposed to an environment with a known moisture concentration. In practice, it is often desired to remove surface contaminants, including moisture, before process steps like optical thickness measurement or deposition of polysilicon for gate stack formation. The mechanistic model can also be used to design an optimum process for removal of adsorbed moisture or estimate the time required to reduce the surface moisture concentration to a desired level by temperature programmed thermal desorption. An example of the profiles generated using the rate parameters is shown in Figures 11 and 12. It is assumed that the three dielectric surfaces are exposed to an atmosphere containing 0.2% moisture at 24°C. The simulated adsorption profiles for all three surfaces are given in Figure 11. As expected, ZrO_2 has the highest surface concentration followed by HfO_2 and SiO_2. This prediction is compatible with our experimental data and is reflected in the adsorption and desorption rate constants estimated from the model. To facilitate thermal desorption, the temperature of the three surfaces is assumed to be ramped from 24 to 325°C at a ramp rate of 5°C/s. Figure 12 shows the desorption concentration profiles generated using the model for the given temperature program. The time required to remove moisture from ZrO_2 and HfO_2 surfaces is clearly higher than that from SiO_2 surfaces. This result is a direct consequence of the desorption rate constants of ZrO_2 and HfO_2 being lower than that of SiO_2. The time estimated to reduce the surface concentration to 1×10^{14} molecules/cm^2 is about 6–7 min for HfO_2 and ZrO_2 surfaces, whereas it is only 60 s for SiO_2. Thus, SiO_2 surfaces can be cleaned faster by thermal desorption, whereas cleanup of HfO_2 and ZrO_2 surfaces before a critical processing step can be a challenge. This exercise further emphasizes the susceptibility of the new high-*k* gate dielectric materials to moisture contamination.

Conclusions

The kinetics and mechanism of adsorption and desorption on high-*k* dielectric surfaces depend on the chemical and crystallographic nature of the substrate as well as the surface preparation and the extent of moisture coverage. The experimental results provide information on the dynamics of adsorption and desorption process on SiO_2, HfO_2, and ZrO_2. The results compare the interactions of moisture with these three oxides in terms of total loading, energetics of adsorption/desorption, and the potential moisture control issues related to these dielectrics. HfO_2 and ZrO_2 surfaces exhibit more affinity for moisture compared to that of SiO_2. The higher affinity of these surfaces is attributed to their higher polarities. A multilayer model is developed to represent the dynamics of adsorption/desorption under nonequilibrium conditions. The model is applicable to a wide range of adsorption/desorption conditions. Desorption kinetics on HfO_2 and ZrO_2 are slower than that on SiO_2; the moisture desorption energy is highest on ZrO_2. Results ob-

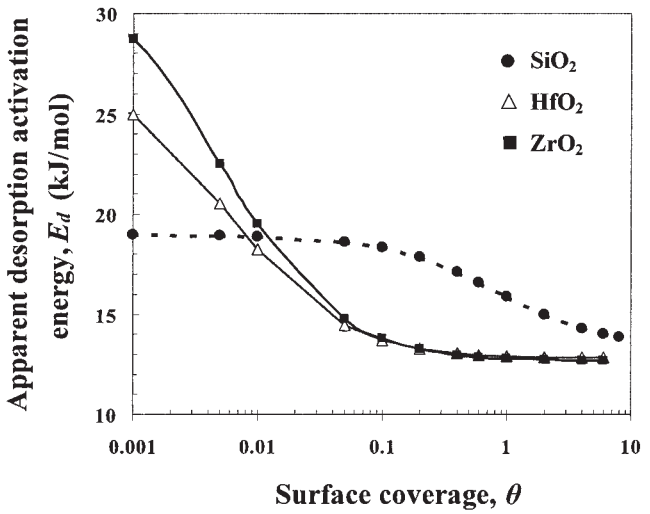

Figure 10. Dependency of apparent activation energy of desorption on surface coverage.

The solid lines are drawn through the data points to show the trend.

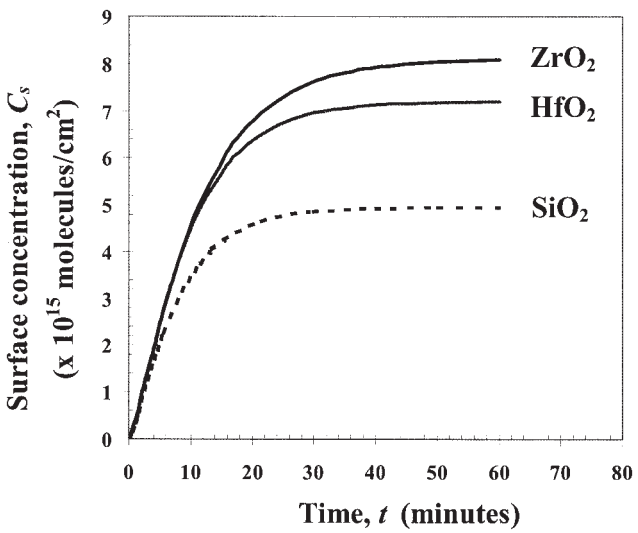

Figure 11. Simulated adsorption concentration profiles at 24°C for 0.2% moisture.

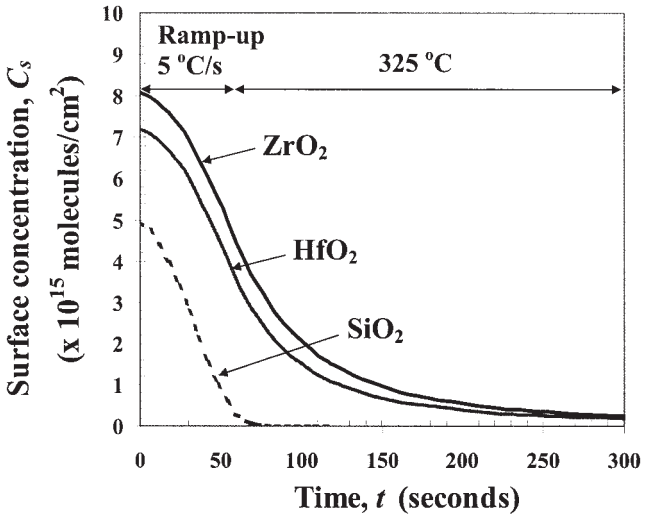

Figure 12. Simulated desorption concentration profiles for a given temperature program.

tained in this study suggest that HfO_2 and ZrO_2, as new alternate dielectric materials, are more prone to moisture contamination compared to SiO_2.

Acknowledgments

The authors are thankful to NSF/SRC Engineering Research Center for Environmentally Benign Semiconductor Manufacturing for partial support of this research, to ASM America for their assistance with the preparation of HfO_2 and ZrO_2 films, and to Intel Corporation for providing the silicon wafers. ALCVD™ is a trademark of ASM International.

Notation

C_g = gas-phase concentration
C_s = surface concentration
C_{s0} = surface concentration to form a monolayer
E_{a1} = adsorption activation energy of moisture influenced by surface interactions
E_{a2} = adsorption activation energy of moisture not influenced by surface interactions
E_d = apparent desorption activation energy
E_{d1} = desorption activation energy of moisture influenced by surface interactions
E_{d2} = desorption activation energy of moisture not influenced by surface interactions
k_a = apparent adsorption rate constant
k_{a1} = adsorption rate constant of moisture influenced by surface interactions
k_{a2} = adsorption rate constant of moisture not influenced by surface interactions
k_d = apparent desorption rate constant
k_{d1} = desorption rate constant of moisture influenced by surface interactions
k_{d2} = desorption rate constant of moisture influenced by surface interactions
p = vapor pressure
p_0 = saturation vapor pressure
R_a = rate of adsorption
R_d = rate of desorption
T = temperature
t = time variable
θ = surface coverage

Literature Cited

Anderson, J. H., and G. A. Parks, "Electrical Conductivity of Silica Gel in the Presence of Adsorbed Water," *J. Phys. Chem.*, **72**, 3662 (1968).
Anderson, J. H., and K. A. Wickersheim, "Near Infrared Characterization of Water and Hydroxyl Groups on Silica surfaces," *Surf. Sci.*, **2**, 252 (1964).
Balog. M., M. Schieber, M. Michman, and S. Patai, "The Chemical Vapor Deposition and Characterization of ZrO_2 Films from Organometallic Compounds," *Thin Solid Films*, **41**, 247 (1977).
Conley, J. F., Jr., Y. Ono, D. J. Tweet, W. Zhuang, M. Khaiser, and R. Solanki, "Preliminary Investigation of Hafnium Oxide Deposited via Atomic Layer Chemical Vapor Deposition (ALCVD)," *IEEE Int. Integrated Reliability Workshop Final Report*, Piscataway, NJ, p. 11 (2001).
Dultsev, F., S. Repinsky, V. Kruchnin, M. Baklanov, and E. Chernakov, "The Change of Properties of Dehydroxylated SiO_2 Layer Surface During Gas Adsorption in the Temperature Range 20–400°C," *Mater. Lett.*, **11**, 119 (1991).
Frpiat, J. J., A. Jelli, G. Poncelet, and J. Andre, **"**Thermodynamic Properties of Adsorbed Water Molecules and Electrical Conduction in Montmorillonites and Silicas," *J. Phys. Chem.*, **69**, 2185 (1965).
Iller, R. K., *The Chemistry of Silica*, 2nd Edition, Chapter 6, Wiley, New York (1979).
Kang, L., B. H. Lee, W. J. Qi, Y. J. Jeon, R. Nieh, S. Gopalan, K. Onishi, and J. C. Lee, "Highly Reliable Thin Hafnium Oxide Gate Dielectric," *Mater. Res. Soc. Symp. Proc.*, **592**, 81 (2000).
Lee, S. J., H. F. Luan, W. P. Bai, C. H. Lee, T. S. Jeon, Y. Senazaki, D. Roberts, and D. L. Kwong, "High Quality Ultra Thin CVD HfO_2 Gate Stack with Poly-Si Gate Electrode," *IEDM Technical Digest*, p. 31 (2000).
Lo, S. H., D. A. Buchanan, Y. Taur, and W. Wang, "Quantum-Mechanical Modeling of Electron Tunneling Current from the Inversion Layer of Ultra-Thin Oxide nMOSFETs," *IEEE Electron. Device Lett.*, **18**, 209 (1997).
Morita, M., H. Fukomoto, T. Imura, Y. Osaka, and M. Ichihara, "Growth of Crystalline Zirconium Dioxide Films on Silicon," *J. Appl. Phys.*, **63**, 2407 (1985).
Peri, J. B., and A. L. Hensley, Jr., **"**The Surface Structure of Silica Gel," *J. Phys. Chem.*, **72**, 2926 (1968).
Raghu, P., N. Rana, C. Yim, E. Shero, and F. Shadman, "Adsorption of Moisture and Organic Contaminants on Hafnium Oxide, Zirconium Oxide, and Silicon Oxide Gate Dielectrics," *J. Electrochem. Soc.*, 150, F186 (2003).
Rana, N., P. Raghu, and F. Shadman, "Kinetics and Mechanisms of Carbon Incorporation in Silicon-Based Ultra-Thin Dielectric Films," *J. Electrochem. Soc.*, **149**(5), F35 (2002).
Rana, N., P. Raghu, E. Shero, and F. Shadman, "Interactions of Moisture and Organic Contaminants with SiO_2 and ZrO_2 Gate Dielectric Films," *Appl. Surf. Sci.*, **205**, 160 (2003).
Sindorf, D. W., and G. E. Maciel, "Solid-State NMR Studies of the Reactions of Silica Surfaces with Polyfunctional Chloromethylsilanes and Ethoxymethylsilanes," *J. Am. Chem. Soc.*, **105**, 1487 (1983).
Sneh, O., M. A. Cameron, and S. M. George, "Adsorption and Desorption Kinetics of H_2O on a Fully Hydroxylated SiO_2 Surface," *Surf Sci.*, **364**, 61 (1996).
Sneh, O., and S. M. George, "Thermal Stability of Hydroxyl Groups on a Well-Defined Silica Surface," *J. Phys. Chem.*, **99**, 4639 (1995).
Takeda, S., M. Fukawa, Y. Hayashi, and K. Matsumoto, "Surface OH Group Governing Adsorption Properties of Metal Oxide Films," *Thin Solid Films*, **339**, 220 (1999).
Vanquickenborne, L. G., *Intermolecular Forces*, Springer-Verlag, Berlin, p. 37 (1991).
Young, G., and T. Bursh, "Immersion Calorimetry Studies of the Interaction of Water with Silica Surfaces," *J. Colloid Sci.*, **15**, 361 (1960).
Zaborski, M., A. Vidal, G. Ligner, H. Balard, E. Papirer, and A. Burneau, "Comparative Study of the Surface Hydroxyl Groups of Fumed and Precipitated Silicas. I. Grafting and Chemical Characterization," *Langmuir*, **5**, 447 (1989).

Manuscript received May 30, 2003, and revision received Nov. 11, 2003.